NASA TECHNICAL NOTE

NASA TN D-2733

NASA TN D-2733

LABORATORY EXPERIMENTS ON THE PERFORMANCE OF SILICON SOLAR CELLS AT HIGH SOLAR INTENSITIES AND TEMPERATURES

by Phillip A. Johnston

Ames Research Center

Moffett Field, Calif.

NATIONAL AERONAUTICS AND SPACE ADMINISTRATION • WASHINGTON, D. C. • MARCH 1965

LABORATORY EXPERIMENTS ON THE PERFORMANCE OF SILICON SOLAR CELLS AT HIGH SOLAR INTENSITIES AND TEMPERATURES

By Phillip A. Johnston

Ames Research Center
Moffett Field, Calif.

NATIONAL AERONAUTICS AND SPACE ADMINISTRATION

For sale by the Office of Technical Services, Department of Commerce,
Washington, D.C. 20230 -- Price $1.00

LABORATORY EXPERIMENTS ON THE PERFORMANCE OF SILICON SOLAR CELLS AT HIGH SOLAR INTENSITIES AND TEMPERATURES

By Phillip A. Johnston

Ames Research Center
Moffett Field, Calif.

SUMMARY

Experiments were conducted to evaluate the performance of silicon solar cells at high temperatures and incident solar energies. The solar cells tested were silicon N/P type with a manufacturer's efficiency rating of 12 percent. Each cell was equipped with a protective cover slide.

The quantum efficiency of each cell was measured at various wavelengths and at temperatures ranging from 303° to 463° K. These measurements were made in accordance with a method perfected by Bell Telephone Laboratories for correlating the laboratory experiments with projected outer space performance. Power output variations due to changes in the angle of incidence have also been measured.

Test results are presented on the basis of distance from the sun. The maximum power output is predicted for a solar cell approaching the sun at angles of 0°, 45°, 60°, and 80°. It appears that silicon solar cells could be used near the sun when inclined at large angles to the incident solar energy. For example, at an angle of 80°, it is estimated that the silicon solar cells tested could approach the sun to within approximately 0.2 astronomical unit without exceeding an assumed upper limiting temperature of 463° K.

INTRODUCTION

To predict the performance of power systems for future space probes, knowledge of solar cell performance over a broad temperature and incident solar energy range is necessary. For example, in a recent feasibility study of a solar probe mission (ref. 1), the possible use of silicon solar cells as the on-board electrical power was considered. For this mission, the space vehicle was to carry scientific instruments to within 1/4 of the earth's distance from the sun. The success of such a mission, in large part, depended upon the distance of closest approach the vehicle could attain and still produce adequate power for the instruments.

A large amount of silicon solar cell performance data was available for the feasibility study. However, the problem was that no common reference was used by the various investigators for solar cell performance in outer space. Different light sources had been used in obtaining the data. The spectral content of these sources did not provide an accurate match of the spectral content of the sun outside the earth's atmosphere, therefore, the solar cell performance for the example mission could be predicted only qualitatively.

The motivation for the current program, then, was the experimental determination of solar cell performance at the temperatures and energies encountered during this typical mission. For this program, a recently reported method developed by Messrs. Gummel and Smits of Bell Telephone Laboratories (ref. 2) was used. This method first required the determination of the solar cell's outer-space short-circuit current. The output characteristics of the test cell could then be measured under any light source whose intensity had been adjusted to produce the predetermined outer-space short-circuit current.

TEST APPARATUS AND PROCEDURE

In this test program, each cell's response was first measured at various wavelengths and temperatures; a standard tungsten lamp was used as the light source. This quantity was then used in conjunction with the zero-air-mass solar spectrum to calculate the outer-space short-circuit current for the test cell. The cell was then placed in the beam of a xenon light source, the intensity of which was adjusted until the cell produced the predetermined outer-space short-circuit current; then, the cell's volt-ampere curve was determined. Another light source, a solar simulator, was used in determining the test cell's power output variations with angle of incidence. In this section, the apparatus utilized in these tests is first described, and then a more detailed discussion of the test procedure is given.

Test Apparatus

Solar cells.- The solar cells tested were silicon N/P type (HTA-106) with an efficiency of 12 percent as rated by the manufacturer, the Heliotek Corporation.[1] Each cell had electroless nickel ohmic contacts and was equipped with a 6-mil glass cover with ultraviolet and antireflective coatings (OCLI 208 SCC 435-2-1.16). The over-all dimensions of each cell, including contacts, were 1 cm by 2 cm, as shown in figure 1(a). The active area of each cell was 1.8 cm^2. For determination of cell temperature, a chromel-constantan thermocouple was pressure-contacted to the negative contact area with a single-component epoxy cured at 280° F, as shown in figure 1(b). The effect of cure temperature on the power output of each cell was found to be negligible by measurements before and after cure.

[1]The junction depth and bulk resistivity were 0.5 micron and 10 Ωcm, respectively.

Equipment used for lamp calibration and solar cell quantum efficiency measurements.- In order to obtain the quantum efficiency of the silicon solar cells, it was necessary to measure the current generated by a known amount of light at various wavelength bands over the wavelength range from 0.4μ to 1.4μ. For this, the current through a 1-ohm resistor connected to the cell's positive and negative terminals was measured.

Light of known intensity over this wavelength range was provided by a tungsten lamp, General Electric Co. type GE 30A/T24/7. This lamp was first calibrated against secondary "standards of spectral irradiance" lamps from the National Bureau of Standards.

The equipment is shown in figure 2 and includes the following: (a) lamp with support stand, (b) mirror, (c) filter wheel, and (d) potentiometer-galvanometer readout equipment. The slit and the detector are partially hidden from view behind the filter wheel.

The mirror had a diameter of 8 inches and a focal length of 42 inches. The reflectance of the mirror, as measured, was approximately 90 percent over all wavelengths considered. The filter wheel contained 20 band-pass filters, each with a bandwidth of 0.1μ. A 0.05μ separation was maintained between the peak transmission wavelengths of adjacent filters over the range from 0.4μ to 1.0μ; a 0.1μ separation was maintained from 1.0μ to 1.5μ. Two detectors were used to cover the wavelength range of interest. A photomultiplier provided detection from 0.4μ to 0.6μ, while a solar cell heated to 423° K covered the interval of 0.5μ to 1.5μ.

After the lamp had been calibrated by comparison with the N.B.S. standard lamps, the same equipment was used to determine the quantum efficiency of the solar cell. For this, the solar cell under test replaced the detector behind the slit.

Other light sources.- The light source used to determine the power output characteristics of the test solar cells at various intensities and temperatures was a Spectrolab Model A-9090 xenon light source. This incorporates an Osram type XBO 1600 xenon arc lamp, the output of which is focused on a test cell by means of an aspheric lens.

The light source for power output measurements as a function of angle of incidence was a model D-1203 Spectrosun, manufactured by the Spectrolab Corporation, which provided a simulated spectrum of zero air mass solar radiation at 1 A.U. (i.e., at 1 astronomical unit, the earth's distance from the sun). The incident intensity of the Spectrosun was established at 140 mw/cm^2 by varying the intensity until the calibration current of a secondary "standard" solar cell was attained. This cell had been calibrated against a standard solar cell (Table Mountain, corrected for zero air mass).

Cell heating equipment.- Each solar cell was placed in a specially designed holder, labelled a in figure 3. A heater element was imbedded in a 1-inch-thick copper block (not shown in the figure). Two 1/4-inch-thick, grooved slabs of boron nitride, which insulated the solar cell against shorting, held the cell in place on the copper block. The cell holder was then

supported on an adjustable rod in the focal plane of the light beam. The micrometer slit (b) and tungsten lamp (c) are also shown in this photograph. This same holder was used with each light source.

Miscellaneous readout equipment.- The short-circuit current measurements utilized in the determination of quantum efficiency were obtained by detecting the voltage drop across a 1-ohm resistor with a precision potentiometer in series with a galvanometer.

Volt-ampere curves were recorded automatically on an X-Y recorder by means of the circuit arrangement shown in figure 4. In essence, the circuit provides a bias voltage which drives the recorder through $X = 0$ when $Y = \max$ and $Y = 0$ when $X = \max$ for the current (Y) and voltage (X), respectively.

Test Procedure

The outer-space power output characteristics of the test cells were determined with the method successfully used by Bell Telephone Laboratories for the solar power plant of the Telstar spacecraft (ref. 3). This method requires no restrictions on the spectral distribution of the light source with which the test cells are illuminated (other than that it produces light at wavelengths to which the cells respond). This method requires precise knowledge of the amount of current generated in the solar cell by a known amount of light at a particular wavelength. This quantity, known as quantum efficiency, is defined in reference 2 as the wavelength-dependent ratio of the number of electrons delivered into a short circuit to the number of photons incident on the cell.

Quantum efficiency is defined herein as

$$Q_i = \frac{I_{sc}(i)}{F_i} \tag{1}$$

where $I_{sc}(i)$ is the short-circuit current in milliamperes produced by the test cell as a result of the amount of light, F_i, in milliwatts which is passed by a particular filter, i. (A complete list of symbols and the units used is presented in the appendix.)

Thus, since the photon flux of the sun has been measured with considerable accuracy at the earth's distance from the sun (as noted in ref. 4), all that remains is to multiply the quantum efficiency at each wavelength by the incident solar photon flux at each wavelength and integrate in order to obtain the outer-space short-circuit current. According to referenc 2, the outer-space short-circuit current, I_{scos}, can be written as

$$I_{scos} = a \int_{\lambda} Q(\lambda) E_{\lambda} \, d_{\lambda} \tag{2}$$

In this instance, E_λ is the solar photon flux in $mw/cm^2\mu$, and a is area of the solar cell in cm^2, and $Q(\lambda)$ is the curve faired through the measured Q_i data points defined in equation (1). The quantum efficiency measurements were also carried out at various temperatures over the range from 303° to 463° K.

A reference condition which is uniquely characteristic of a particular solar cell can be determined from equation (2), that is, the maximum current that can be generated by the solar cell for a particular temperature and incident intensity. Any source having sufficient intensity to generate this value of short-circuit current in the solar cell can now be used to establish the outer-space power output of the test cell as indicated in reference 3. Thus, if a test cell is placed in a beam of light and the incident intensity is adjusted until the cell produces the previously calculated value of outer-space short-circuit current, then by increasing the load resistance (see circuit diagram in figure 4) and monitoring the voltage and current simultaneously, one obtains the volt-ampere characteristic typical of that cell in outer space. It is then only a matter of applying Ohm's law to obtain the power output from this curve.

The above is a general discussion of the experimental measurements and the accompanying calculations required in going from a quantum efficiency measurement using a tungsten lamp to the prediction of power output of a solar cell in outer space. The test procedure for the individual measurements follows, accompanied by a general discussion of the accuracy of the measurements as applied to the accuracy with which the outer-space power output was predicted.

Quantum efficiency.- As previously stated, the quantum efficiency of a solar cell is determined by measuring the current generated by a solar cell exposed to a known amount of monochromatic light, as indicated in equation (1).

The incident photon flux, F_i, through a given filter from a standard tungsten lamp is calculated from the following relationship derived from general solid-angle aperture considerations, as suggested by the National Bureau of Standards in their bulletin, "Instructions for Using the Standards of Spectral Radiance":

$$F_i = R_i L_i \frac{sA}{D^2} \tag{3}$$

where L_i is the radiance after transmission through one of the spectral filters; R_i (averaged over the region where L_i is defined) and A are the reflectance and surface area, respectively, of the 8-inch-diameter mirror previously mentioned in the apparatus section of this report; s is the area of the slit; and D is the distance from the mirror to the slit.

The transmission through each filter is the product of L_λ and $\tau_\lambda(i)$, the spectral radiance of the calibrated lamp and the transmittance of the filter, respectively. Thus, the transmitted radiance in equation (3) is

$$L_i = \int_{\lambda} L_\lambda \tau_\lambda(i)\, d\lambda \qquad (4)$$

The cell to be tested was positioned behind the micrometer slit, so that all of the light passing through the slit was incident on the solar cell. After adjusting the solar cell in the light beam to get maximum current, the cell holder was locked in place. The various filters were then placed in the beam and the short-circuit current at each wavelength, $I_{sc}(i)$, was determined. The quantum efficiency, Q_i, was subsequently computed. This procedure was repeated at each equilibrium temperature. Each solar cell's equilibrium temperature was determined by measuring the voltage applied in nulling the galvanometer deflection resulting from the voltage generated by its thermocouple.

Power output.- The output characteristics (V-I curve) of each test cell were measured as follows: after the intensity of the xenon light source was adjusted until the cell produced the predetermined outer-space short-circuit current at the prescribed solar cell temperature, the load across the cell was varied and the volt-ampere curve recorded.

The power output was measured as a function of angle of incidence in the following manner: each cell was placed on the cell holder. The holder was placed in a movable frame which was supported on a rigid stand. A protractor was fixed to the movable frame such that as the angle of the cell to the incident light beam was varied, the angle was indicated by a pointer attached to the stand. The holder was subsequently placed in the Spectrosun beam, the intensity of which had been previously set by means of the calibrated secondary standard solar cell. The volt-ampere curves were then determined as described above from the normal to an 80° angle of incidence.

Accuracy of the method.- The accuracy with which the power output in outer space can be predicted by this method is determined by the accuracy with which Q_i is determined, as well as the accuracy with which the photon flux of the sun has been determined. These two factors determine the reference outer-space short-circuit current. Once a cell is generating this current, it becomes necessary to determine the accuracy with which the volt-ampere curve, as well as the cells temperature, is measured.

It is estimated that the cumulative error in the determination of Q_i should not exceed ±3 percent, and the error encountered in the V-I curve measurement should be less than 2 percent. Thus, there should be no greater than ±5-percent error in the determination of quantities based upon experiments reported herein. The errors due to inaccuracies in temperature measurements were also considered and found to be negligible. With an assumed error of ±3 percent in the determination of solar photon flux, the performance of these solar cells in outer space would be estimated to be within ±8 percent of the values predicted.

RESULTS AND DISCUSSION

The results of this experimental program will be presented in the order used to predict the outer-space maximum power output of the silicon solar cells tested. First, the quantum efficiencies measured at various temperatures for the test cells will be discussed. This will be followed by a discussion of the utilization of these quantum efficiencies in the calculation of the outer-space short-circuit current. Then, the measured volt-ampere curves, based on the calculated outer-space short-circuit current, will be discussed. Finally, after predicting the solar cell's temperature at various distances from the sun, the estimated maximum power output of the test cell will be presented as a function of distance from the sun.

It will be observed that the highest temperature for which test results are presented throughout this report is 463° K. This temperature was the upper limit of operation for the combination of solar cell, solder, and lead wires used, since throughout the tests performed on the solar cells, more than one-half of the cells failed at this temperature because of loss of the soldered electrical connections to the cell.

Quantum Efficiency

Figure 5 shows the quantum efficiencies, Q_i, as a function of wavelength at 303°, 355°, 407°, 438°, and 463° K for an N/P type solar cell. A shift toward the infrared in each silicon solar cell's quantum efficiency curve was observed when the temperature was increased from 303° to 463° K. At 303° K, the peak of the faired curve occurred at approximately 0.85μ; and at 463° K, it was approximately 0.95μ. As pointed out in reference 5, this effect is attributed to a shift to longer wavelengths in the optical absorption of silicon. A calculation was carried out to determine at what wavelengths the maximum carrier generation in silicon would occur for temperatures of 303° and 463° K. This quantity was calculated using the shift in optical absorption for each temperature, as predicted by Fan et al. (ref. 6). The wavelength at which the maximum quantum efficiency occurred for both temperatures corresponded to the wavelengths at which the maximum carrier generation occurred for those same temperatures.

Calculation of Outer-Space Short-Circuit Current

Figure 6 illustrates the variation of outer-space short-circuit current of the test cell with temperature and incident intensity as computed from equation (2). In this case

$$E_\lambda = \frac{E_\lambda'}{\bar{r}^2} \tag{5}$$

represents the inverse square law dependence of incident solar energy on distance, $\bar{r}$, and E_{λ}' is the solar photon flux at 1 A.U. (see ref. 4).

It is seen from figure 6 that an increase in outer-space short-circuit current of about 15 percent is encountered when the equilibrium temperature of the solar cell is increased from 303° to 463° K. This is probably due to an increase in minority carrier diffusion length as observed by various other investigators.

Power Output

Temperature and intensity effects.- Figure 7 shows four typical volt-ampere curves produced by adjusting the incident intensity of the xenon light source until the test cell was generating the value of outer-space short-circuit current as calculated from equation (2). The sensitivity of short-circuit current to changes in source intensity, as well as the sensitivity of open-circuit voltage to changes in temperature, is well illustrated. The combined effects on power output are observed as changes in the maximum power points of the curves.

The test parameters and the corresponding results obtained in the measurement of these and other volt-ampere curves are listed in table I. A complete set of the measured volt-ampere curves is available, upon request, from the author. The maximum power points are presented for various temperatures and intensities in figure 8. It should be noted particularly that, at a given solar energy, the cell output decreases significantly as the cell temperature increases.

Angular variations.- The effect of varying the angle of incidence on the maximum power output of a solar cell has been measured at a total photon flux of 140 mw/cm^2. The large reductions in measured power output could not be accounted for merely by multiplying the cosine of the incident angle times the power output at normal incidence. This is shown in figure 9 where the angular degradation factor, K, obtained from the following relationship

$$K = \frac{P_{max}(\theta)}{[P_{max}(\theta \text{ normal})]\cos \theta} \tag{6}$$

is plotted as a function of the angle of incidence. The decrease in K is significant at angles greater than 60°. The reason for this effect has not been thoroughly studied, however, the power degradation due to changes in radiation intensity, such as that described in reference 7, has been considered and found to be relatively small in this case. For example, at $\theta = 0$, a 10-percent deviation in linearity of power output with intensity was observed when the intensity was reduced to 20 mw/cm^2 by means of neutral density filters. Thus, it is assumed that the observed effect is primarily due to changes in the reflective characteristics of the cell at high angles of incidence.

Solar Cell Temperature in Outer Space

The temperature of a solar cell at a point in space is determined by its ability to absorb and reject heat originating from the incident solar energy. This ability is determined by the configuration of the structure which carried the cell and by the material from which the structure is made.

A change in the solar absorptance of the cell, comparable to the change of angular degradation factor (see fig. 9), should be expected as the angle to the incident solar flux is increased, based on the aforementioned assumption that the deviation from the cosine law is due to changes in the reflective properties of the cell. This consideration is contained in the following equation from reference 8 which has been modified here by the angular degradation factor, K.

$$T^4 = \frac{\alpha_S}{\epsilon_S + \epsilon_B} \frac{E}{\bar{r}^2} \frac{\cos \theta}{\sigma} K \qquad (7)$$

The temperatures of a solar cell affixed to the paddle of a vehicle, similar to the concept of a solar probe (ref. 1), have been calculated for various distances from the sun and are shown in figure 10 for paddle orientations to the incident solar energy of 0°, 45°, 60°, 70°, and 80°. The values of σ, ϵ_S, ϵ_B, and α_S are given in the list of symbols. The effect of the angular degradation factor K (fig. 9) on the solar cell temperature is also illustrated in figure 10 for the angles 60°, 70°, and 80°. It is seen that the distance from the sun at which the solar cell would attain the assumed 463° K limiting temperature has been considerably reduced by incorporating the angular degradation factor in the determination of cell temperature.

Power Output in Outer Space

The maximum power output of a typical test cell on a fixed paddle of a vehicle at various distances from the sun is shown in figure 11. These curves are obtained from the data of figures 8 and 9 and the calculated curves of figure 10. Power outputs for cell temperatures computed from cosine law dependence, K = 1 in equation (7), as well as for those modified by the angular degradation factor, are illustrated. In each case, the distance of closest approach to the sun at a given angle of incidence has been established by the limiting temperature of 463° K, as previously mentioned. The combined effects of temperature and intensity on power output are illustrated. It should be noted at this point that a potentially important factor, the effect of time at elevated temperature on power output of the cell has not been taken into account in the current study. That is, in these experiments the solar cells were at elevated temperatures for periods of less than 24 hours; whereas, in space during a mission of the solar-probe-type considered, the cells could be at elevated temperatures for periods of weeks to months.

It is observed in figure 11 that, for any fixed paddle orientation, the power output first increases as the distance from the sun decreases, then cell performance begins decreasing rather abruptly as the detrimental effect of high temperature overcomes the beneficial effect of the increased intensity. As indicated earlier, at high angles to the incident solar energy, the characteristics of the cell that lead to the angular degradation factor actually have a beneficial effect on power output when the cell is near the sun. This is indicated in figure 11 where at $\theta = 80^\circ$, for example, the allowable distance of closest approach to the sun is 0.16 rather than 0.20 A.U. since $K = 0.55$ rather than 1. Although not apparent from this figure, it should be noted that temperatures as low as 185° K (-88° C) could be experienced by a solar cell inclined to an angle of 80° at the earth's distance from the sun. Such low temperatures might cause structural problems due to thermal stresses in solar cell, bond, substructure system. If a programmed variation of the inclination of the paddles to the solar flux is considered, then an essentially constant power output could be achieved into about 0.2 A.U., and the possible low-temperature problem just mentioned would be reduced.

CONCLUDING REMARKS

As a solar cell approaches the sun, it encounters an increase in solar radiation intensity which increases its temperature. Thus, the initial increase in solar cell power output with the increase in intensity is eventually counteracted by a decrease because of the detrimental effect of high temperature.

The distance of closest approach to the sun could be improved if the solar cell were deflected to some fixed angle with respect to the incident solar energy, however, there would be a consequent loss in power output at the earth's distance from the sun. Also, it was found that the cell could approach the sun significantly closer than expected for a given temperature limit if the assumed reflective characteristics of the cell at high angles of incidence reduced the temperature increase. It should be emphasized that this effect was determined only for the cells tested. It is expected that there could be substantial differences in this effect due to differences in coatings, protective cover glasses, and solar cells.

A relatively constant power output to a vehicle would be possible if the solar paddles were designed so that their angle to the incident solar energy could be gradually increased as the vehicle approached the sun. This would overcome the condition of low power output at the earth's distance from the sun for high angles to the incident solar energy.

Ames Research Center
National Aeronautics and Space Administration
Moffett Field, Calif., Sept. 24, 1964

APPENDIX

SYMBOLS

A	area of spherical mirror, cm^2
a	area of the solar cell, cm^2
D	distance from the mirror to the slit, cm
E	total incident solar flux, mw/cm^2
E_λ	solar energy, $mw/cm^2\mu$
E_λ'	solar energy, $mw/cm^2\mu$ (ref. 4) at 1 A.U.
F_i	photon flux, mw
I_{sc}	short-circuit current, ma
$I_{sc}(i)$	wavelength dependent short-circuit current, ma
I_{scos}	outer-space short-circuit current, ma
i	filter number
K	angular degradation factor
L_λ	spectral radiance of calibrated lamp, $\frac{mw}{\mu} \frac{1}{cm^2 \text{ steradian}}$
L_i	transmitted radiance of calibrated lamp, mw/cm^2 steradian
P_{max}	maximum power output at normal incidence, mw
$P_{max}(\theta)$	maximum power output at any angle θ, mw
Q_i	quantum efficiency, ma/mw
$Q(\lambda)$	curve faired through the measured Q_i data points defined in eq. (1)
R_i	reflectance of the spherical mirror averaged over the region where L_i is defined
$\bar{r}$	distance from the sun, A.U. (1 A.U. = 93,000,000 mi.)
s	area of the slit, cm^2

T	temperature, ^{o}K
V_{oc}	open-circuit voltage, v
α_s	solar absorptance of the solar cell, 0.87 (ref. 7)
ϵ_B	emittance of the solar cell back surface, 0.85 (ref. 7)
ϵ_s	emittance of the solar cell front surface, 0.87 (ref. 7)
θ	angle of incident light
λ	wavelength, microns
σ	Stefan-Boltzmann constant, 5.67×10^{-9} $mw/cm^2(^{o}K)^4$
$\tau_\lambda(i)$	spectral transmittance of ith filter

REFERENCES

1. Hall, Charles F., Nothwang, George J., and Hornby, Harold: Solar Probes. Aerospace Engineering, vol. 21, no. 5, May 1962, pp. 22-30.

2. Gummel, H. K., and Smits, F. M.: Solar Power System Calibration and Testing. Rep. PIC-SOL-209/2.1, Proc. of the Solar Working Group Conference of the Interagency Advanced Power Group, sec. 3, vol. II, April 1962.

3. Smith, K. D., Gummel, H. K., Bode, J. D., Cuttriss, D. B., Nielson, R. J., and Rosenzweig, W.: The Solar Cells and Their Mounting. Bell System Tech. Jour., vol. XLII, no. 4, pt. 3, July 1963, pp. 1765-1817.

4. Johnson, Francis S.: The Solar Constant. Jour. of Meteorology, vol. 11, no. 6, Dec. 1954, pp. 431-9.

5. Moss, T. S.: Optical Properties of Semi-Conductors. Academic Press, N. Y., 1959.

6. Fan, H. Y., Shepherd, M. L., and Spitzer, W.: Infrared Absorption and Energy Band Structure of Germanium and Silicon. Photoconductivity Conference, Breckenridge, R. G., ed., John Wiley and Sons, Inc., N. Y., 1956, pp. 184-203.

7. Prince, M. B., and Wolfe, M.: New Developments in Silicon Photovoltaic Devices. Jour. of British I.R.E., vol. 18, Oct. 1958, pp. 583-595.

8. Evans, W. H., Mann, A. E., Weiman, I., and Wright W. V.: Solar Panel Design Considerations. Space Power Systems, Academic Press, N. Y., 1961, pp. 79-110.

TABLE I.- TEST RESULTS

T, °K	E, mw/cm²	θ, deg	I_{sc}, ma	V_{oc}, v	P_{max}, mw
313	140	0	65	0.580	27.9
↓	↓	20	61	.578	26.3
		30	56.5	.570	24.25
		40	49.0	.567	20.90
		50	40.0	.560	17.05
		60	30.0	.553	12.60
		70	19.0	.540	7.86
		80	7.0	.510	2.65
303		0	65	.538	24.00
355		↓	65.5	.405	16.00
407			66	.300	10.00
438			67	.230	6.50
463	↓		73	.190	4.00
303	220		97	.540	34.00
↓	390		174	.550	55.00
	600		265	.551	70.00
355	220		103	.415	24.65
↓	390		177	.428	37.60
	600		278	.430	49.00
407	220		103	.312	15.00
↓	390		183	.322	23.00
	600		275	.332	31.00
438	220		105	.240	10.00
↓	390		188	.252	15.00
	600	↓	285	.263	22.50

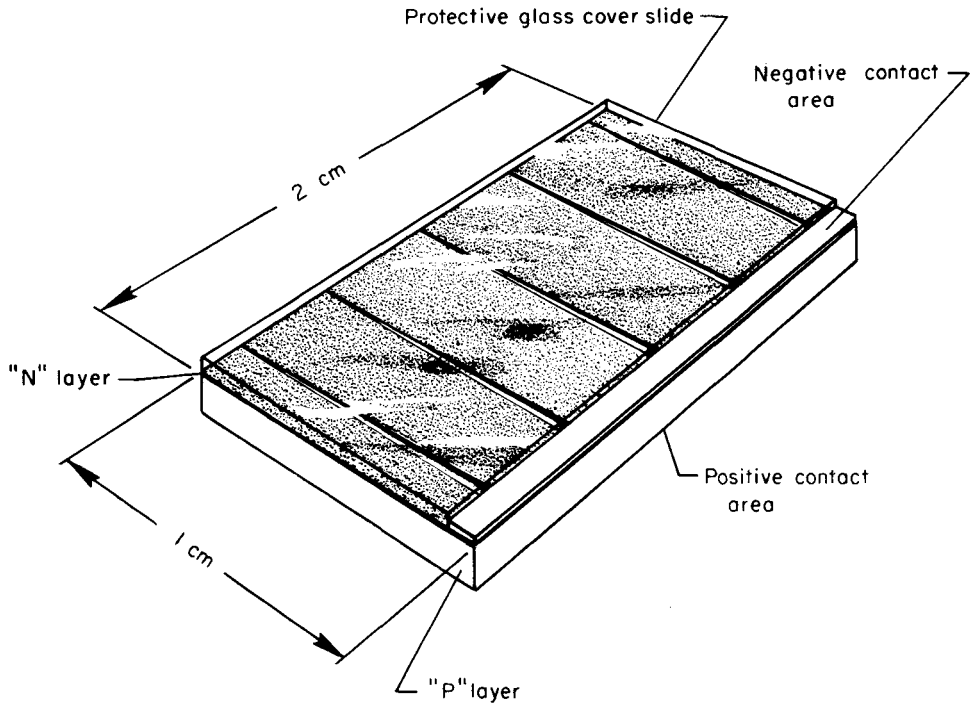

(a) Solar cell.

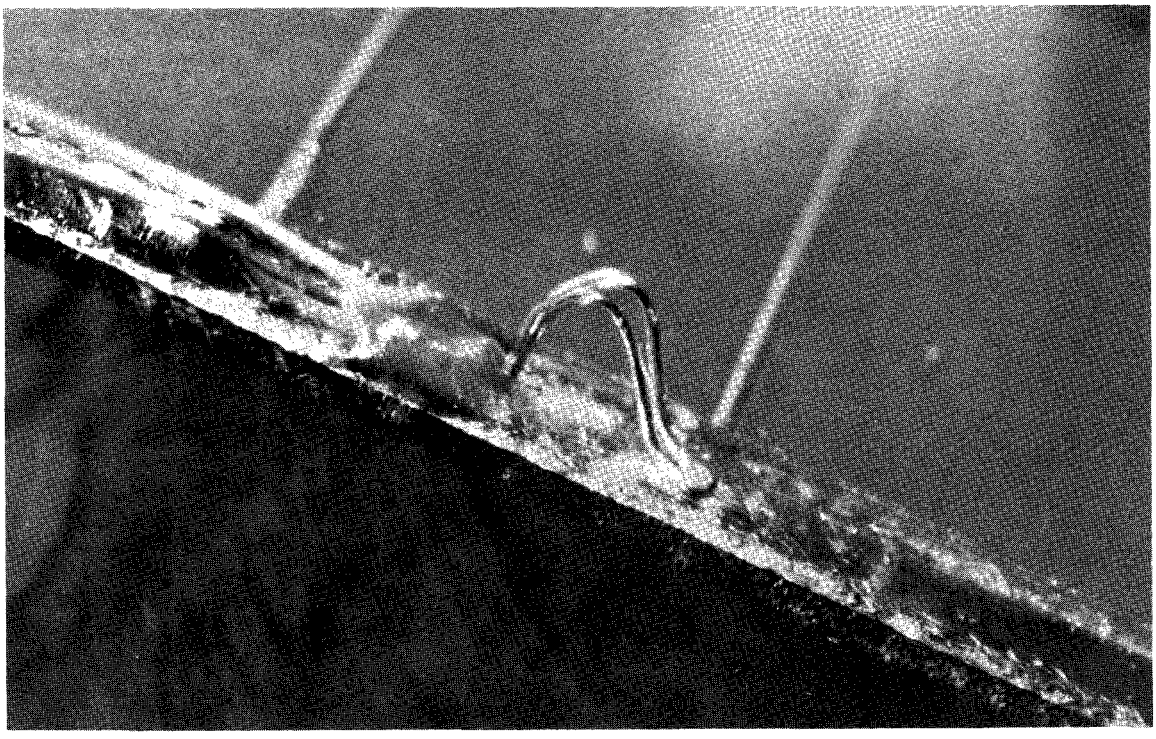

A-30300

(b) Thermocouple bonded to solar cell.

Figure 1.- Typical solar cell.

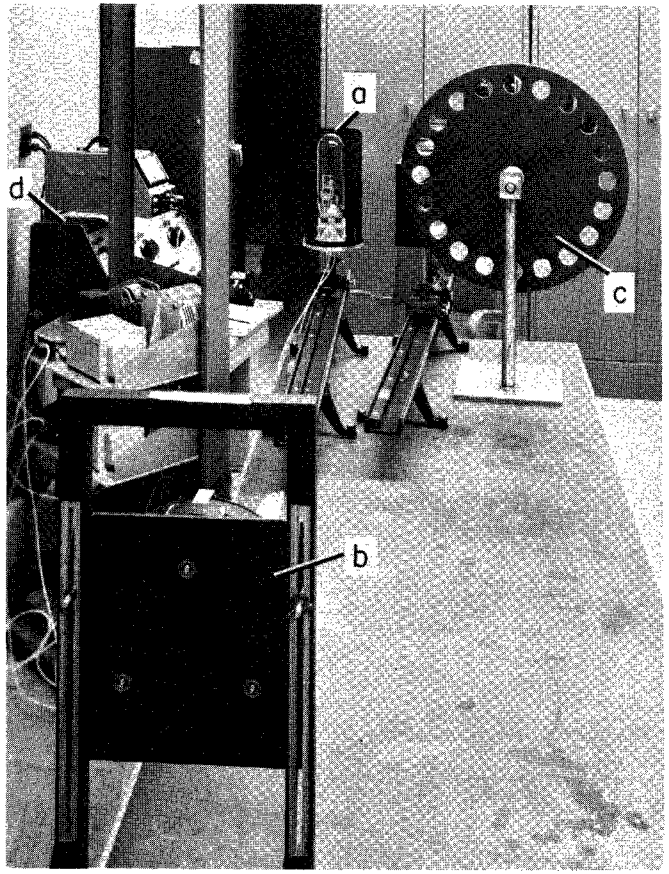

A-30299.1

Figure 2.- Lamp calibration equipment.

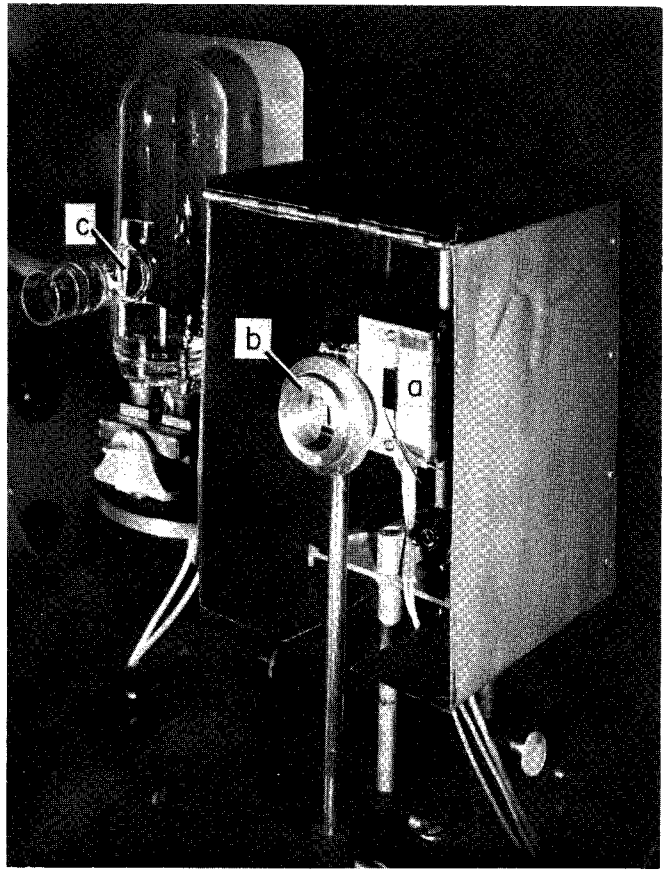

A-30298.1

Figure 3.- Solar cell holder and associated components.

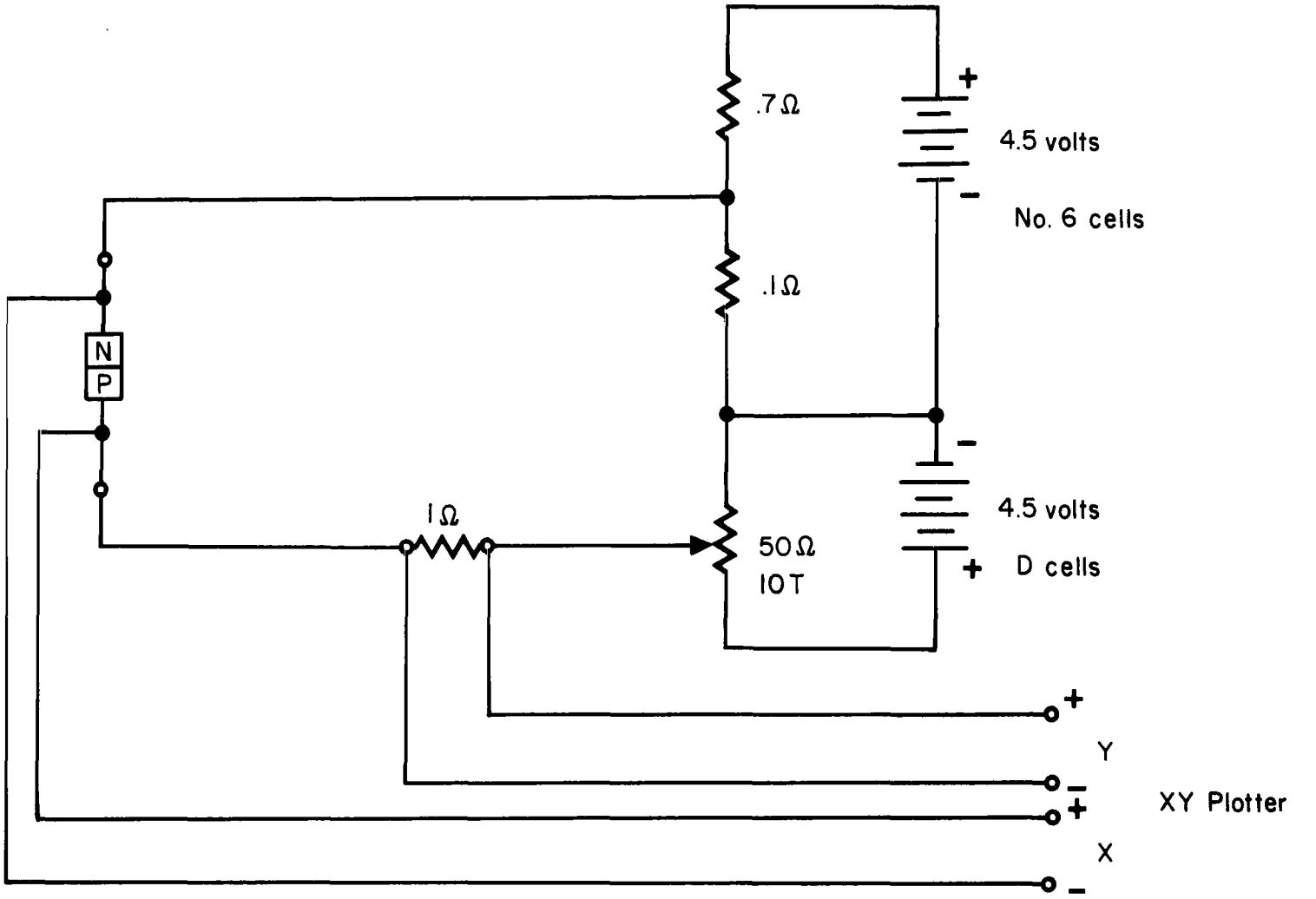

Figure 4.- Circuit diagram for volt-ampere curve determination.

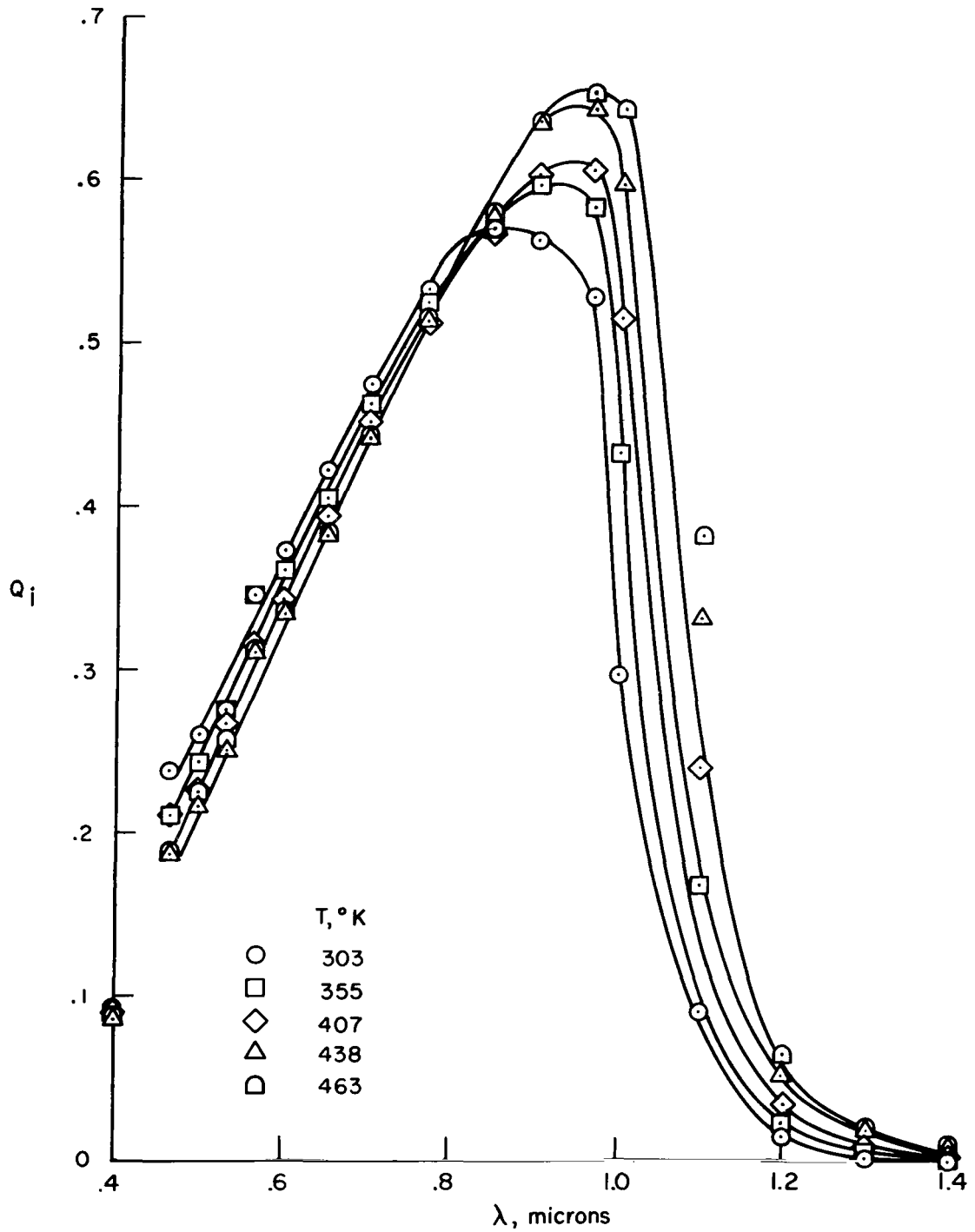

Figure 5.- Quantum efficiencies measured at various temperatures using a standardized tungsten lamp.

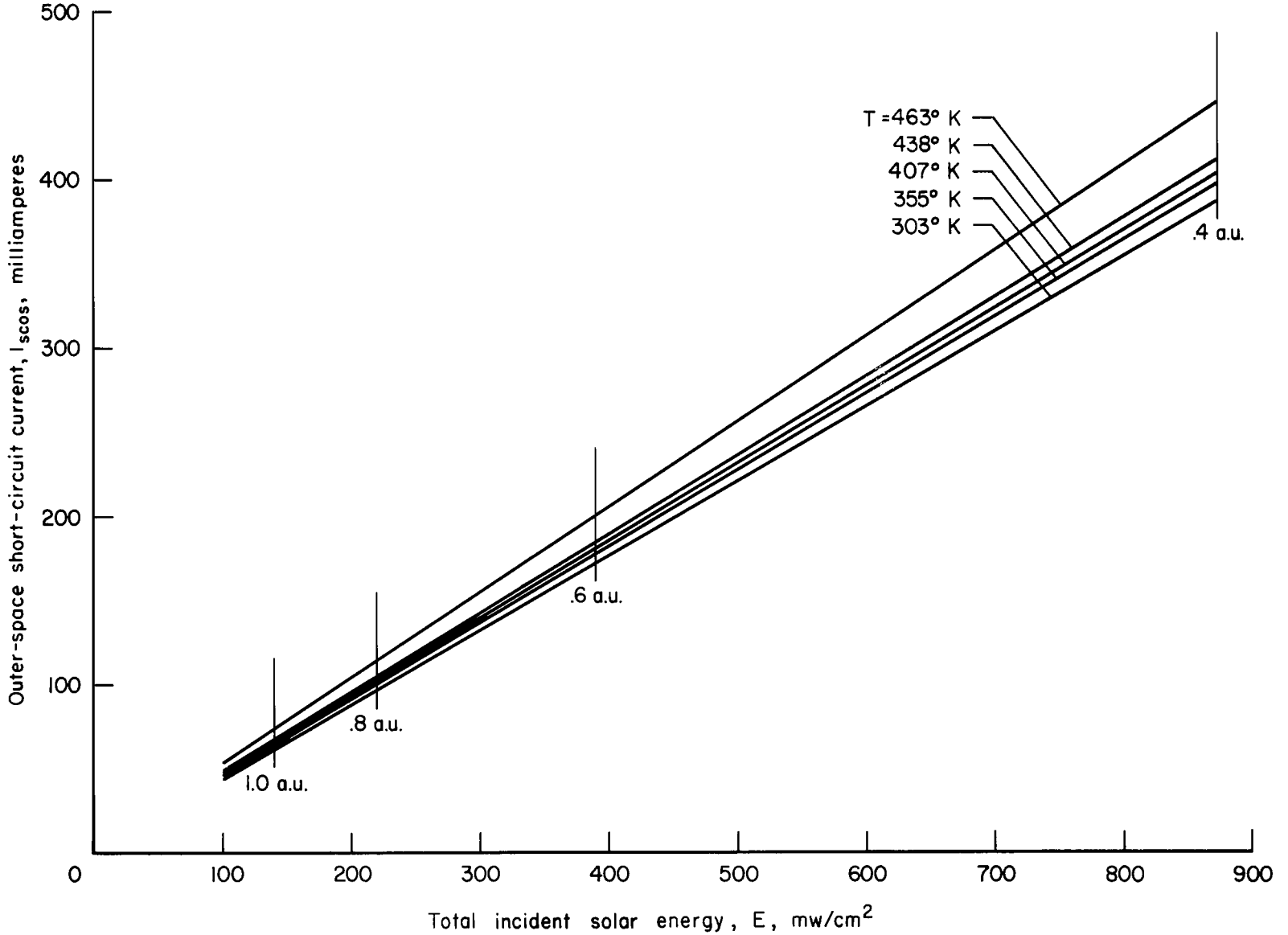

Figure 6.- Variation of outer-space short-circuit current with solar energy for various solar cell temperatures.

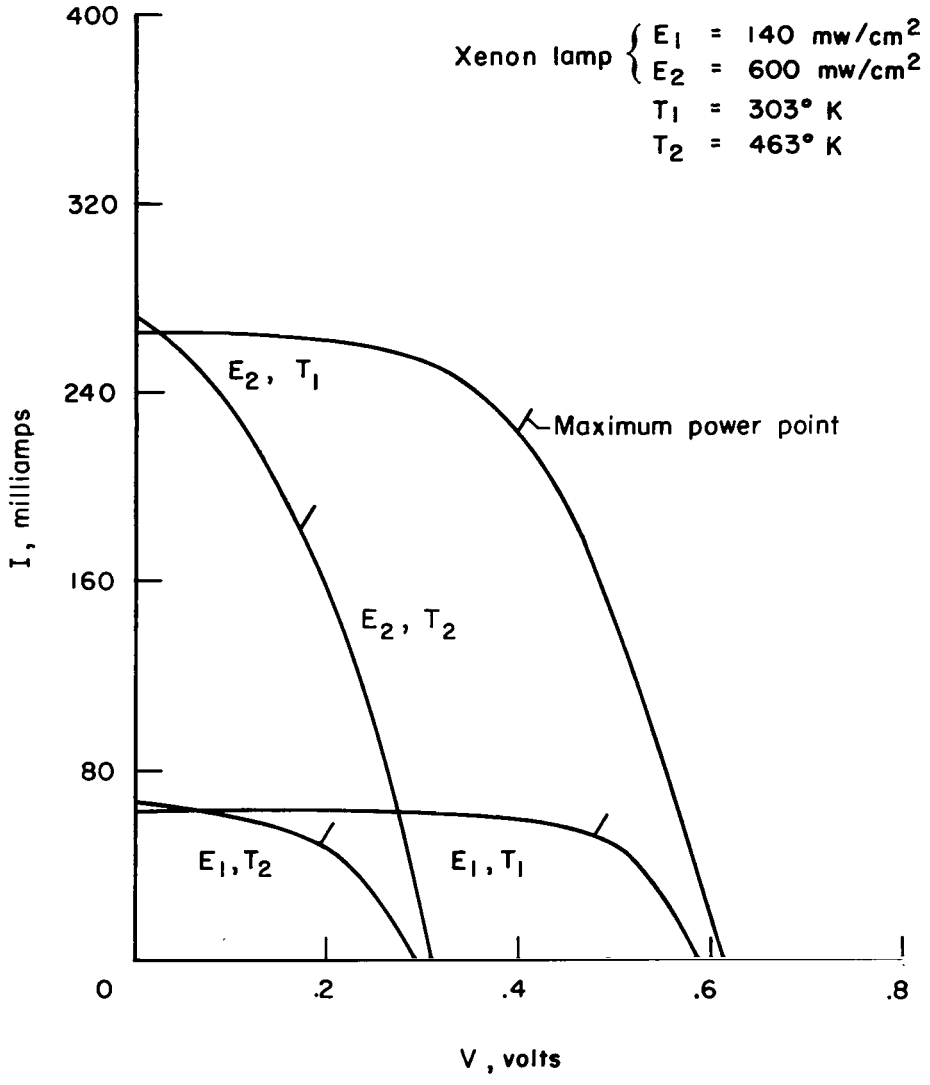

Figure 7.- Typical measured volt-ampere curves.

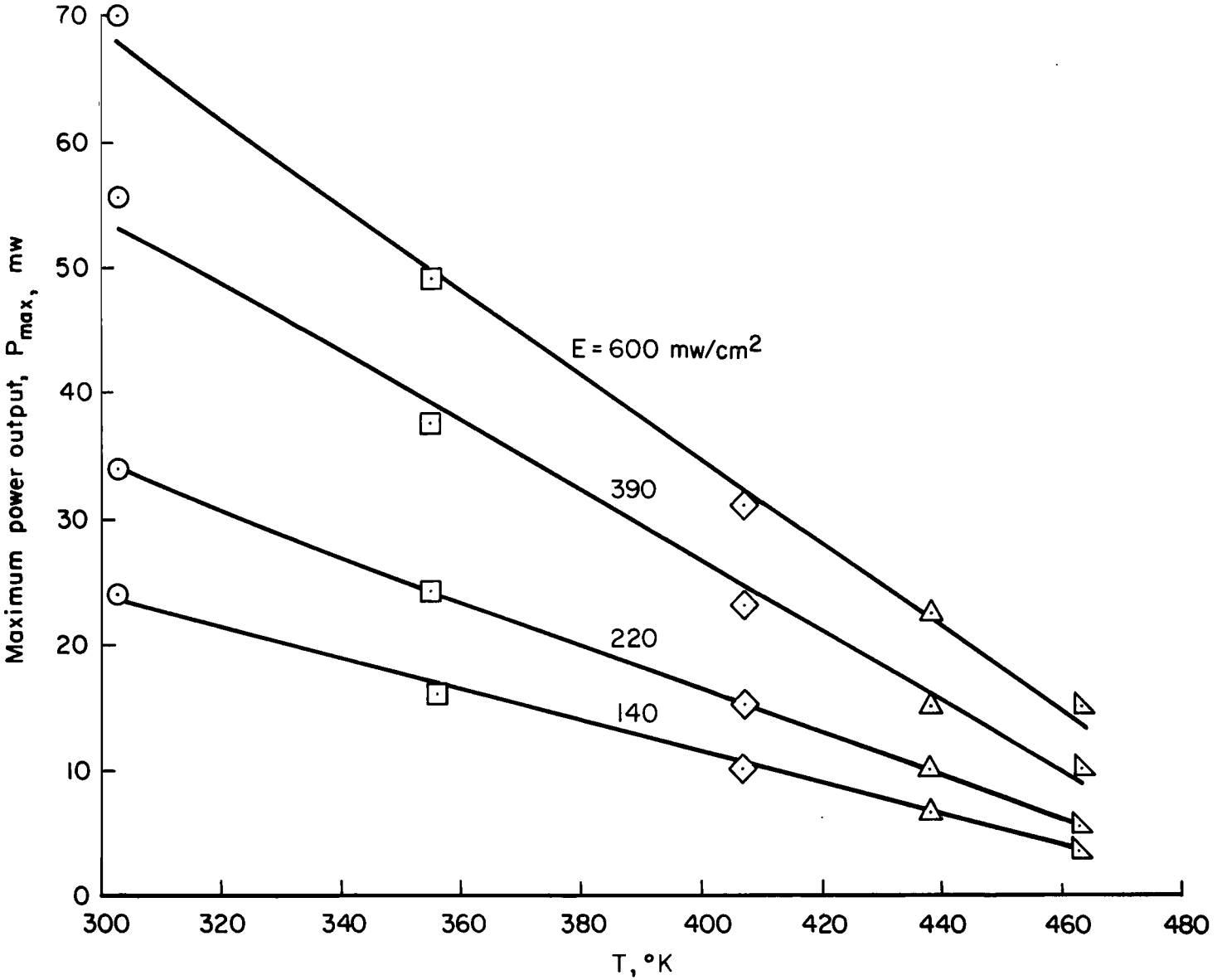

Figure 8.- Changes in outer-space power output for various combinations of temperature and incident solar energy.

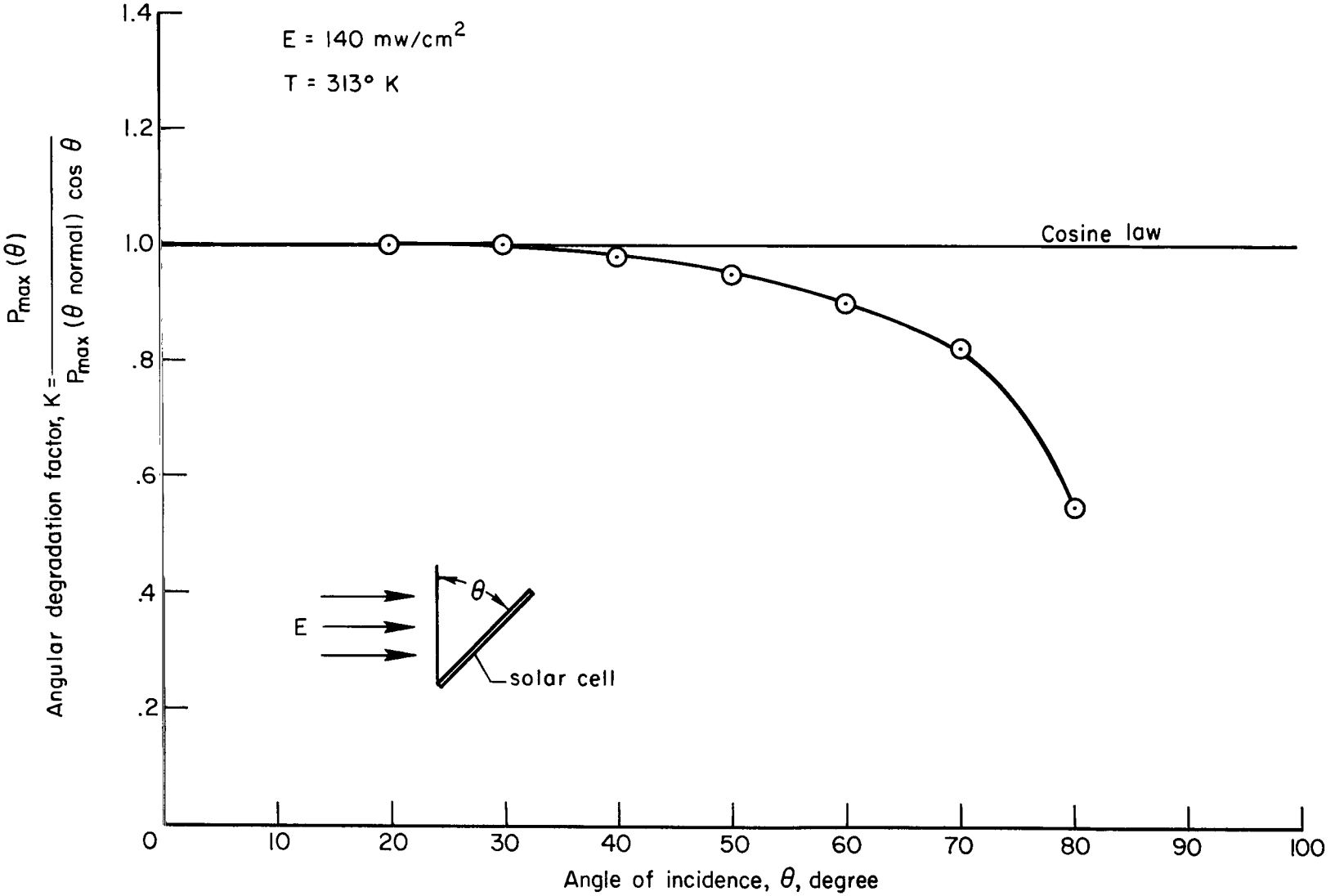

Figure 9.- Deviation from the cosine law of power output with the angle of incident solar energy.

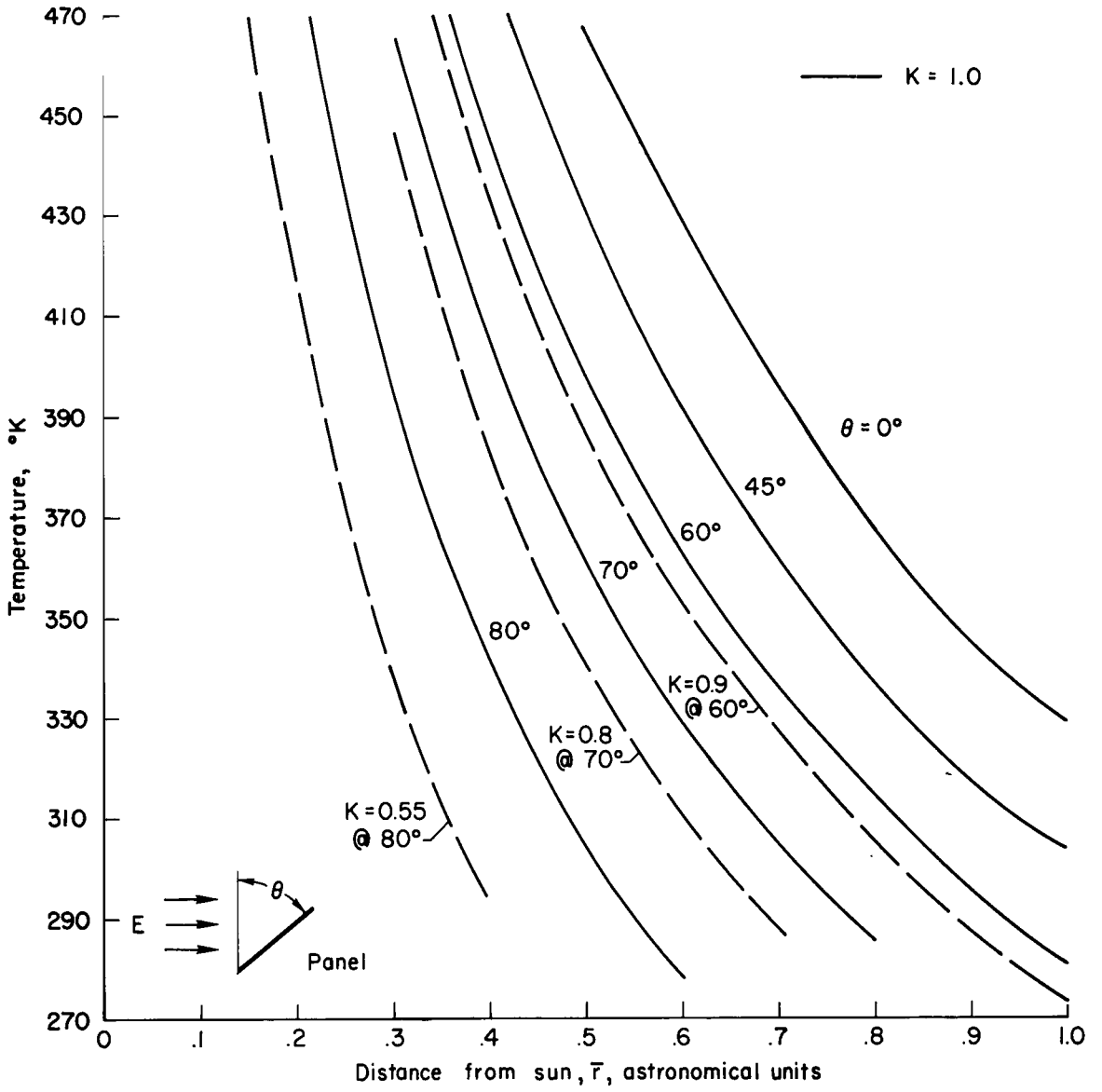

Figure 10.- Silicon solar cell temperature at various distances from the sun for various angles to the incident solar energy.

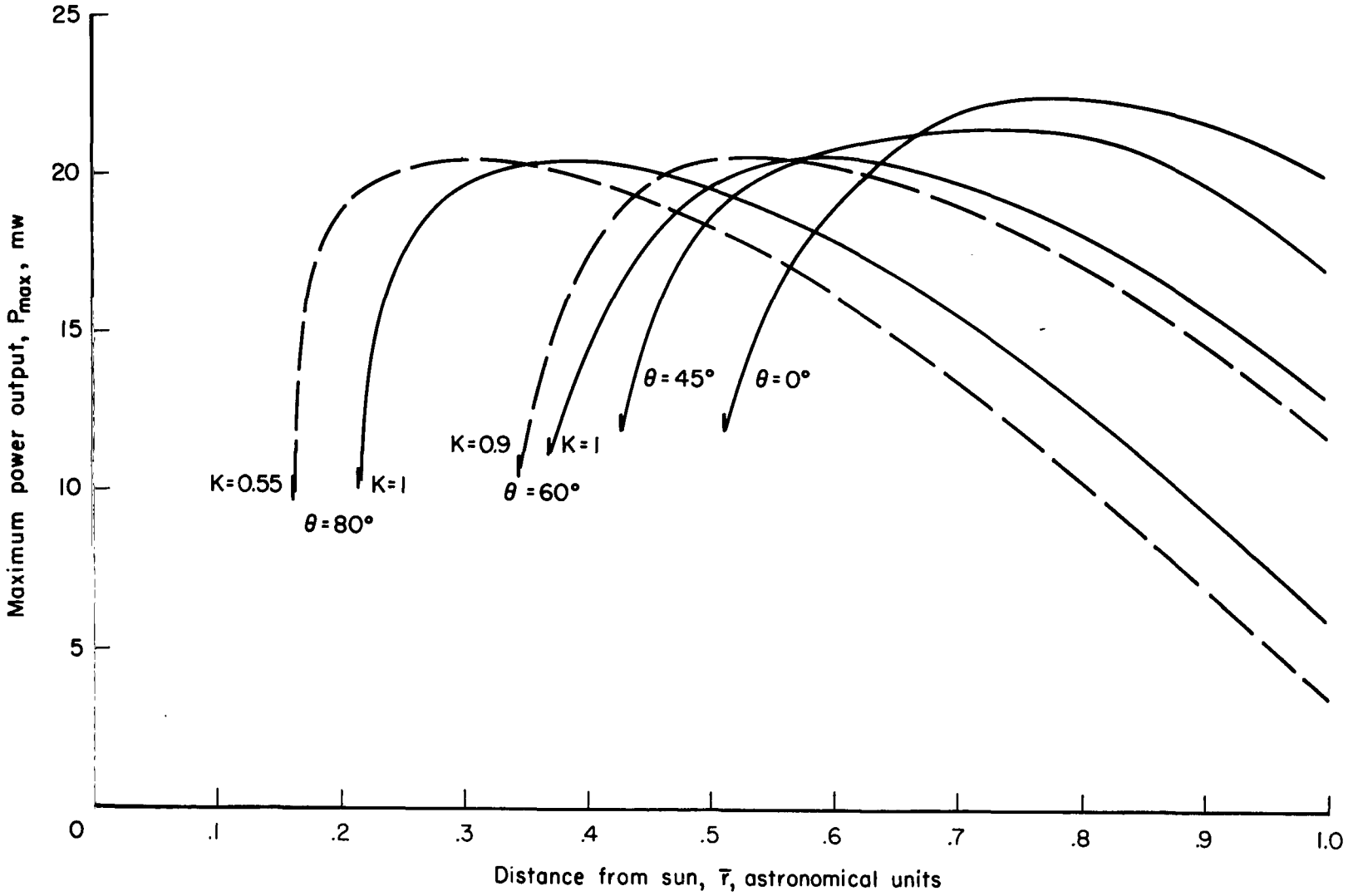

Figure 11.- Power output of a silicon solar cell at various distances from the sun and at various angles to the incident solar energy.

2/22/85

"The aeronautical and space activities of the United States shall be conducted so as to contribute . . . to the expansion of human knowledge of phenomena in the atmosphere and space. The Administration shall provide for the widest practicable and appropriate dissemination of information concerning its activities and the results thereof."

—NATIONAL AERONAUTICS AND SPACE ACT OF 1958

NASA SCIENTIFIC AND TECHNICAL PUBLICATIONS

TECHNICAL REPORTS: Scientific and technical information considered important, complete, and a lasting contribution to existing knowledge.

TECHNICAL NOTES: Information less broad in scope but nevertheless of importance as a contribution to existing knowledge.

TECHNICAL MEMORANDUMS: Information receiving limited distribution because of preliminary data, security classification, or other reasons.

CONTRACTOR REPORTS: Technical information generated in connection with a NASA contract or grant and released under NASA auspices.

TECHNICAL TRANSLATIONS: Information published in a foreign language considered to merit NASA distribution in English.

TECHNICAL REPRINTS: Information derived from NASA activities and initially published in the form of journal articles.

SPECIAL PUBLICATIONS: Information derived from or of value to NASA activities but not necessarily reporting the results of individual NASA-programmed scientific efforts. Publications include conference proceedings, monographs, data compilations, handbooks, sourcebooks, and special bibliographies.

Details on the availability of these publications may be obtained from:

SCIENTIFIC AND TECHNICAL INFORMATION DIVISION

NATIONAL AERONAUTICS AND SPACE ADMINISTRATION

Washington, D.C. 20546